

Direnzoite, $[\text{NaK}_6\text{MgCa}_2(\text{Al}_{13}\text{Si}_{47}\text{O}_{120})\cdot 36\text{H}_2\text{O}]$, a new zeolite from Massif Central (France): Description and crystal structure

E. GALLI AND A.F. GUALTIERI*

Dipartimento di Scienze della Terra, Università di Modena e R.E., Via S.Eufemia 19, I-41100 Modena, Italy

ABSTRACT

The crystal structure of direnzoite, a new natural zeolite found in the cavities of a xenolithic rock from the Massif Central (France) is reported. Apparently, direnzoite was formed throughout a process of hydrothermal crystallization within the vugs of a highly porphyric basalt. The determination of the crystal structure of this new zeolite was at the limits of the existing experimental techniques because of the paucity of available specimen, mainly composed of three tiny aggregates of fibrous microcrystals. The structure of direnzoite, solved by powder methods, was shown to be the K-dominant equivalent of the synthetic zeolite ECR-1 with a framework composed of layers of mordenite (MOR) and mazzite (MAZ) connected in a regular 1:1 stacking sequence with assigned framework topology EON. The chemical composition of direnzoite determined from the structure refinement is $(\text{Na}_{0.94}\text{K}_{6.62}\text{Mg}_{1.42}\text{Ca}_{2.24})(\text{Si},\text{Al})_{60}\text{O}_{120}\cdot 36.8\text{H}_2\text{O}$. The unit cell determined from the Rietveld structure refinement is $a = 7.57887(18) \text{ \AA}$, $b = 18.20098(57) \text{ \AA}$, $c = 26.15387(83) \text{ \AA}$, and the space group is *Pmnn*.

Six extra-framework sites and 14 water molecules were identified within the zeolite micropores. Three extra-framework sites are occupied by K^+ ions. The others are occupied by Na^+ , Ca^{++} , and Mg^{++} . Although direnzoite and ECR-1 share the same framework, the distribution of their extra-framework cations is rather different. In direnzoite, there are no equivalent positions to C1, C2, and C4 positions found in ECR-1. Only sites C3 and C3b correspond respectively to K3 and Ca in direnzoite. In direnzoite, K1, K2, and Na correspond to water molecules sites ($\text{H}_2\text{O}1$, $\text{H}_2\text{O}11$, and $\text{H}_2\text{O}8$, respectively) in ECR-1.

Keywords: Zeolite, xenolith, synchrotron, powder diffraction, microprobe analysis

INTRODUCTION

More than 30 years ago, during a field trip to Massif Central (France) in search for zeolite minerals, Glauco Gottardi and Ermanno Galli collected a sub-spherical xenolith of nearly 20 cm in diameter, having an extremely curious and distinctive appearance. Later, a preliminary optical inspection revealed that the piece of rock contained many cavities filled with crystals of almost certainly newly formed minerals. The mineralogical characterization (mainly qualitative X-ray diffraction using Gandolfi camera) confirmed the initial guess. Beside well-known mineral species such as zeolites, carbonates, and silicates, the diffraction pattern of small aggregates or a micro-crystalline phase with an apparently fibrous habit appeared to be different from that of all the mineral phases reported in the updated JCPDS crystallographic databases. Since the amount of available material was indeed very small (only three small spherical aggregates of fibrous micro-crystals were available and no single crystals could be separated for the determination of the structure), one of the authors (E.G.) organized three further field trips in the attempt

to find other specimens of this apparently new mineral species. Unfortunately, all the attempts were unsuccessful.

In the meantime, the experimental techniques for the chemical and structural characterization of micro-volume materials have rapidly developed with the advent and development of synchrotron radiation (structure determination from powders is now more or less a routine analysis). Thus, a chance was given to disclose the crystal chemistry of this species and reveal its structure.

The discovery of a new species is a rare event as about a hundred natural zeolites are known to date (Armbruster and Gunter 2001). Thus, the discovery of a new natural zeolite is very important for the mineralogy community. Moreover, it is very useful for the understanding of the chemical stability, formation conditions, and properties of the synthetic counterparts (Gottardi and Galli 1985). Besides the scientific interest, zeolites have unique physical chemical properties (such as molecular sieving, cation exchange, dehydration/rehydration, etc.), which can be used for a nearly infinite number of technological/industrial applications (catalysis, molecular sieving for gas and liquid separation, animal feeding, agriculture, and others). The paramount interest in their technological properties is certainly the impetus to create zeolites in the laboratory. Zeolite synthesis has now become a viable routine practice in many laboratories all

* E-mail: gualtieri.alessandro@unimore.it

over the world and, because the composition of synthetic zeolites may vary more widely (including Ga, Ge, Be, P in place of Si/Al in the framework, and alkali, alkaline-earth, rare earth elements and organic complexes as extra-framework cations) the number of known synthetic zeolites nowadays is by far much larger than that of the natural species.

The mineral data and the proposed mineral name for the new zeolite presented here have been approved (IMA 2006-044) by the Commission on New Minerals and Mineral Names (CNMMN) of the International Mineralogical Association (IMA). The name *direnzoite* was given in honor of Dr. Francesco Di Renzo, born in 1954, Research Director at the Laboratoire de Matériaux Catalytiques et Catalyse en Chimie Organique, Ecole Nationale Supérieure de Chimie de Montpellier (France), a prominent personality and excellent scientist in the field of zeolites, mesoporous materials, and catalysis.

Direnzoite is the K-dominant equivalent of the synthetic zeolite ECR-1 whose structure model was proposed on the basis of HRTEM evidence and structure solution of the synthetic isotype gallo-silicate TNU-7 (Warrender et al. 2005), and confirmed later by Rietveld structure refinement (Gualtieri et al. 2006). The isotopic structures of ECR-1 and *direnzoite* consist of structure layers of mordenite (MOR) and mazzite (MAZ) connected in a regular 1:1 stacking sequence and framework topology EON. Here, this new mineral species and its crystal structure are described.

OCCURRENCE AND SPECIMEN DESCRIPTION

The zeolite specimen was found inside the cavities of a piece of xenolith rock found in the Massif Central, France. This region is characterized by alkaline volcanism, where the basic lavas are composed of alkaline basalts or basanites and may contain analcime, nepheline, and leucite. Early volcanic activity in that region occurred since Mid Jurassic up to Upper Oligocene. The xenolith was collected at Mont Peyrenc, near the town of St. Pierre Eynac, in the volcanic province of Velay. These volcanic rocks belong to the Na-alkaline series with undifferentiated basalts and late end-members, such as phonolites and alkaline trachytes (Brousse 1961). The xenolith was collected from a highly porphyric basalt, whose prominent phenocrysts were olivine, clinopyroxene, and plagioclase. The piece of xenolith, with an approximate diameter of 20 cm, was divided in several parts to allow a more thorough investigation with the optical microscope (Fig. 1). Many cavities were present and hosted a variety of minerals. The specimen is mainly composed of sub-spherical grains of glass (about 70–80%) with a color that varies from ice-white to dark brown and variable size. A thin film of clayey material is also present as substrate. The other minerals composing the rock were sillimanite, cordierite, quartz, feldspar, olivine, plagioclase, pyroxenes, ilmenite, and rutile. The cavities are filled with newly formed minerals grown on the clayey substrate. The following zeolites were recognized: mordenite, phillipsite, merlinoite, erionite, analcime, and chabazite, in addition to calcite and aragonite.

The amount of *direnzoite* in the collected xenolite rock is very minute: only three very small spherical aggregates of fibrous needle-like microcrystals are available. The size of the single aggregates is within 0.3–0.5 mm and the individual acicular crystals



FIGURE 1. A fragment of the original piece of xenolith of about 4 cm diameter that contained the new zeolite specimen. Color view online.

are about 1–5 μm wide and 30–50 μm long. The crystal habit is striated-acicular. SEM images and compositional maps have been collected to disclose the crystal morphology and chemical variability. The images show the appearance of the aggregates at two different scales (Fig. 2). The size of the crystals is very small and they form radially fibrous aggregates that compose more or less a sphere with a diameter of about 300 μm . Such radially fibrous aggregates have been already observed for natural zeolites such as mordenite and phillipsite. Unfortunately, it is not possible to clearly observe the termination of the crystals. The single crystals have a length of about 100 μm , and a base smaller than 10 μm . Due to their size, it is impossible to separate a single crystal for the study of the crystal structure by single-crystal diffraction techniques.

Physical properties

The specimen crystal aggregates are transparent to translucent, colorless with a white streak and vitreous to silky luster. The crystals are non-fluorescent and unfortunately too small to allow a direct measurement of the hardness. Supposedly, the Mohs hardness has the mean value (4.5) between that of mordenite and mazzite because the structure of *direnzoite* consists of layers of mordenite (MOR) and mazzite (MAZ) connected in a regular 1:1 stacking sequence. The crystal habit is fibrous/acicular. Twinning was not observed. The tenacity is brittle and the cleavage is distinct along the [010]. The fracture is splintery and uneven. The density measured by flotation in aqueous solution of potassium iodomercurate is 2.12(3) g/cm^3 . The calculated density (with empirical formula) is 2.080 (5) g/cm^3 . Because of the extremely small size of the crystals and the intrinsic difficulty to handle barely discernable needle crystals, only an overall refractive index was determined using the Becke line method in immersion oils. The value is 1.483(3). The crystals are non-pleochroic.

Three infrared patterns (Fig. 3) were collected with the micro-IR Attenuated Total Reflectance (ATR) technique. Although the signal is disturbed in the 4000–1400 cm^{-1} range because of the extremely small size of the crystal fragments, the main absorption bands are visible. The first band clearly visible is at about 1700

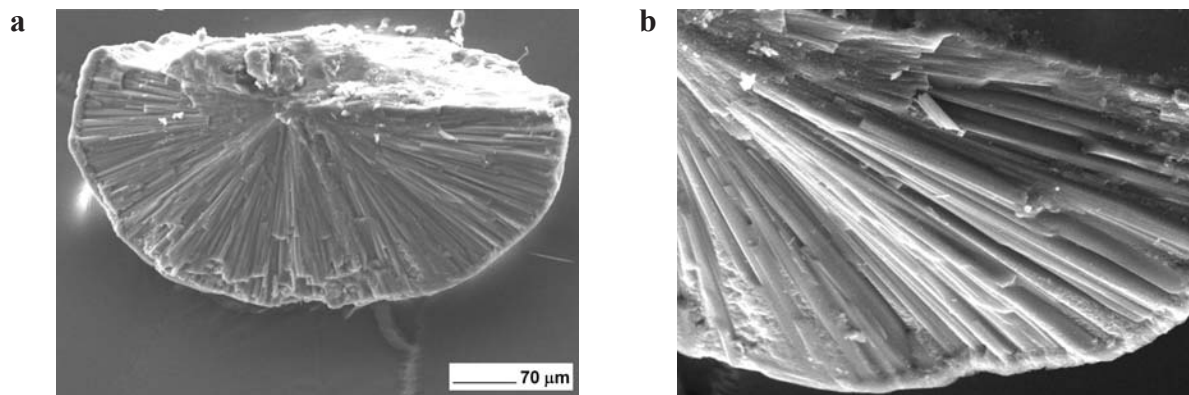


FIGURE 2. Selected SEM micrographs of direnzoite.

cm^{-1} , due to the vibration of water molecules. The highest band shows a minimum between 970 and 1000 cm^{-1} , corresponding to the asymmetric stretch of the T-O bond. Two other bands are visible: (1) the first at 850 cm^{-1} (symmetric stretch of extra-tetrahedral bonds) and (2) the second at 730 cm^{-1} (symmetric stretch of the T-O bond).

Chemical composition

The chemical analysis using a small piece of one aggregate has been obtained by electron microprobe analysis (EPMA). The fragment of the specimen was embedded in an epoxy resin, polished to achieve a smooth surface and coated with a carbon film. Polishing has been performed with 0.25 μm abrasive paste by a Struers DP-U2 instrumentation. Analyses were made using a WDS (wavelength dispersive) system ARL-SEM-Q, with 15 kV and 10 nA and a 30 μm diameter beam. Iron was assumed to be in the ferric state. Only analyses with a balance error E% $\{= 100 \times [(\text{Al}) - (\text{Li} + \text{Na} + \text{K}) - 2(\text{Mg} + \text{Ca} + \text{Fe} + \text{Sr} + \text{Ba})] / [(\text{Li} + \text{Na} + \text{K}) + 2(\text{Mg} + \text{Ca} + \text{Fe} + \text{Sr} + \text{Ba})]$; Passaglia 1970} < 20 were considered. Water was calculated by difference, and confirmed later by the results from the Rietveld structure refinement. In fact, the thermogravimetric analysis was not performed because of the paucity of the sample. The mean analytical results are reported in Table 1. The empirical formula (based on 120 structural oxygen apfu) is:



with a Si/Al ratio of 3.507. Although we cannot rule out an underestimation of Na^+ because of its migration effect under the electron beam, we believe that the large balance error E% = 14.63 is mainly due to the migration of K^+ ions located within the large 12-ring channel under the electron beam. As a matter of fact, the content of K^+ ions determined from the structure refinement is much larger than that found by EPMA, as described below the section on the crystal structure.

Powder pattern

A film (Kodak Industrex MX) of direnzoite collected with a 72 h long exposure using a Gandolfi camera and a Ni-filtered Copper radiation was used for the calculation of the powder pat-

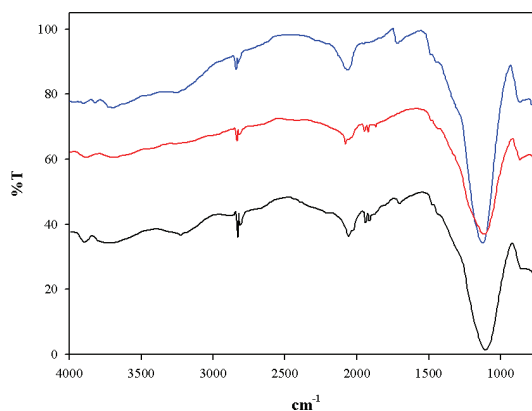


FIGURE 3. Patterns collected from three different spots of the zeolite specimen using the micro-IR Attenuated Total Reflectance (ATR) technique in the 4000–1400 cm^{-1} range. Color view available online.

TABLE 1. Chemical composition of direnzoite

Constituent	Wt%	Range	Stand. dev.	Probe Standard
SiO_2	62.45	60.04–63.78	2.09	natural albite
Al_2O_3	15.11	14.04–16.11	1.04	natural albite
MgO	1.39	1.30–1.52	0.11	D185-JD15
Fe_2O_3	0.27	0.19–0.41	0.12	P140 olivine
CaO	2.69	2.61–2.85	0.14	synthetic An_{70} glass
Na_2O	0.77	0.70–0.82	0.06	natural albite
K_2O	2.85	2.45–3.08	0.35	microcline
BaO	0.04	0.00–0.11	0.06	paracelsian
SrO	0.08	0.02–0.12	0.05	Sr-anorthite
H_2O^*	14.35	11.40–18.54		
Total	100.00			

* By difference.

tern. The powder pattern was obtained by line integration along the equatorial plane of the film, and background subtraction. With the powder pattern from Gandolfi data processed with the program X'Pert HighScore Plus Ver. 2.1.0 (PANalytical B.V.), it was possible to calculate the relative intensity, the observed peak positions and d spacings (see Table 2). A reliable determination of the observed intensities was possible only up to 50 $^\circ 2\theta$. The calculated d spacings and the Miller indices are relative to the unit cell determined from the Rietveld structure refinement [$a = 7.57887(18)$ \AA , $b = 18.20098(57)$ \AA , $c = 26.15387(83)$ \AA] with space group $Pm\bar{m}n$.

TABLE 2. X-ray powder-diffraction data of direnzoite (bold values indicate the most intense reflections)

I_{rel}	2θ	d_{obs} (Å)	d_{calc} (Å)	hkl	I_{rel}	2θ	d_{obs} (Å)	d_{calc} (Å)	hkl
n.d.	n.d.	n.d.	26.154	0 0 1	4.2	38.029	2.366	2.368	2 6 0
10.0	5.920	14.940	14.939	0 1 1				2.367	1 7 3
26.1	6.824	12.953	13.077	0 0 2				2.365	1 6 6
21.6	8.361	10.576	10.620	0 1 2	15.7	39.643	2.273	2.275	0 8 0
60.4	9.744	9.077	9.100	0 2 0				2.275	3 0 5
14.9	10.325	8.568	8.595	0 2 1				2.271	0 5 9
41.1	11.277	7.846	7.862	0 1 3	2.4	40.524	2.226	2.227	2 6 4
8.3	11.890	7.443	7.469	0 2 2				2.226	1 7 5
31.2	13.098	6.760	6.759	1 1 1				2.224	0 6 8
16.5	14.094	6.284	6.295	0 2 3	2.4	41.664	2.168	2.170	3 1 6
29.1	15.025	5.896	5.910	0 3 1				2.164	0 1 12
4.5	16.102	5.504	5.503	0 3 2	5.3	42.362	2.134	2.138	2 1 10
11.4	16.726	5.300	5.310	0 2 4				2.137	2 7 1
20.7	17.728	5.003	5.027	0 1 5				2.134	0 7 7
5.9	18.665	4.754	4.777	1 1 4				2.134	1 6 8
			4.736	1 3 0				2.130	3 3 5
29.5	19.960	4.448	4.447	0 3 4	5.0	43.220	2.093	2.095	2 2 10
44.4	20.981	4.234	4.239	0 1 6				2.095	1 0 12
0.9	22.092	4.024	4.034	0 4 3				2.093	3 0 7
24.4	23.125	3.846	3.854	1 4 1				2.092	3 4 4
			3.836	1 3 4				2.050	3 5 2
30.3	24.304	3.662	3.673	2 1 1	6.9	44.295	2.045	2.047	2 5 8
			3.660	0 1 7				2.045	1 5 10
46.6	25.089	3.549	3.540	0 3 6				2.041	1 2 12
71.4	25.565	3.484	3.490	1 2 6				2.040	3 2 7
19.7	26.242	3.396	3.414	2 1 3	7.5	44.973	2.016	2.017	0 8 6
54.7	27.279	3.269	3.269	0 0 8				2.016	0 9 1
100.0	28.042	3.182	3.190	2 3 1	9.6	45.778	1.982	1.987	3 1 8
			3.183	1 5 2				1.984	2 7 5
			3.181	0 3 7				1.981	0 6 10
			3.180	0 5 4				1.980	1 3 12
16.1	29.015	3.077	3.077	0 2 8	9.1	46.655	1.947	1.948	2 5 9
			3.071	1 5 3				1.946	2 4 10
			3.069	2 0 5	4.0	47.178	1.926	1.929	3 5 5
36.8	29.685	3.009	3.002	1 0 8				1.925	1 5 11
47.5	30.757	2.907	2.912	2 4 0				1.924	2 7 6
			2.908	2 2 5	23.2	48.003	1.895	1.896	3 1 9
			2.907	1 4 6				1.895	3 6 3
			2.906	0 0 9				1.895	4 0 0
7.4	32.150	2.784	2.794	0 5 6	6.4	48.622	1.873	1.875	4 0 2
			2.780	1 5 5				1.874	3 5 6
1.9	32.782	2.732	2.738	2 3 5				1.872	1 9 4
			2.728	2 2 6				1.871	0 6 11
9.8	33.357	2.686	2.690	1 3 8	1.3	49.393	1.845	1.850	2 2 12
			2.684	1 1 9				1.844	0 7 10
			2.680	1 6 3				1.842	4 1 3
18.8	34.620	2.591	2.600	1 2 9				1.842	2 4 11
			2.589	0 1 10				1.840	0 4 13
10.2	36.150	2.485	2.491	3 1 1	9.3	49.999	1.824	1.828	2 8 5
			2.490	0 6 6				1.820	0 10 0
14.5	36.874	2.438	2.436	2 3 7				1.820	3 6 5
				2 5 4				1.820	4 0 4
								1.820	3 3 9

CRYSTAL STRUCTURE

Experimental and structure solution/refinement

The crystal structure solution of direnzoite was possible because it is isotopic with synthetic zeolite ECR-1. Hence the structure model of ECR-1 (Gualtieri et al. 2006) was used for the refinement with the Rietveld method. As previously mentioned, the powder method was used because of the lack of suitable single crystals.

Many attempts to solve this structure by ab initio powder methods with the most advanced software available in the literature for the structure solution of complex structures like zeolites failed supposedly due to (1) the large unit cell with too many independent positions both for the framework and extra-framework atoms, and (2) partial occupancy of most of the extra-framework atomic sites.

For the Rietveld refinement, aggregates of crystals of sub-micrometer size (the average length of the crystals is around 0.5 μm and their average width is around 50–100 nm) were randomly mounted on the tip of a thin glass filament of a goniometer head. Different sets of synchrotron powder-diffraction data were collected at the Italian beamline (GILDA, BM08) at the European Synchrotron Radiation Source (ESRF) in Grenoble (France). The patterns were collected in parallel beam Debye geometry using an Imaging Plate (IP) (Amemija 1990; Me-

neghini et al. 2001) with a λ of 0.688876 Å. The wavelength was calibrated against the NBS-640b Si standard with $a = 5.43094(4)$ Å at 298 K. Full diffraction rings were recorded with an exposure time of 30 min, using an IP detector, mounted perpendicular to the incoming beam at a distance of 235.7 mm. The images stored in the IP were recovered using a scanner with a dynamical range of 16 bit/pixel with a minimum pixel size of $50 \times 50 \mu\text{m}^2$, and transformed into digitalized data reporting the intensity and the peak position using the FIT2D software (Hammersley 1998). Powder data were also collected at the BM01b beamline at ESRF (Grenoble, France) using a Debye-Scherrer geometry. BM01b is installed on a bending magnet source (dipole BM01). A vacuum pipe delivers a 1 mrad fan of radiation (from -11.0 to -12.0 mrad) directly into the hut situated 10 m downstream from a splitter-vessel. A water-cooled, flat-crystal monochromator is positioned after a cooled Be-window. This monochromator is a channel-cut Si (111) crystal. A 2-circle diffractometer and a Debye-Scherrer capillary geometry were used for the measurements. The diffractometer is equipped with six counting chains delivering six complete patterns collected simultaneously, with a small offset in 2θ . A Si-111 analyzer crystal is mounted in front of each detector (Na-I scintillation counter), resulting in an intrinsic resolution (FWHM) of $\sim 0.01^\circ$ at a wavelength of 1 Å. The wavelength used for the experiment was 0.79992 Å calibrated against the Si NIST 640c standard with a certified cell parameter $a = 5.4311946(92)$ Å. The capillary

was spun during the measurements and irradiated by a beam whose size was $4 \times 1 \text{ mm}^2$. Data were collected up to $55^\circ 2\theta$ (maximum $\sin\theta/\lambda$ of about 1.02 \AA^{-1}) with steps of $0.003^\circ 2\theta$ and 3 s/step.

To improve statistics, two independent data sets were collected at each beamline. The simultaneous refinement of the four data sets was performed using the GSAS package (Larson and Von Dreele 2000) and the EXPGUI graphical interface (Toby 2001). As described above, the starting atomic coordinates for the framework atoms only were taken from Gualtieri et al. (2006) and refined in the space group *Pmmn*. The background, manually subtracted in the first data set, was fitted with a Chebyshev polynomial function with a variable number of polynomial coefficients. The profile of the diffraction peaks was modeled using a pseudo-Voigt function with one Gaussian and two Lorentzian coefficients. The refinement of the atomic coordinates, the atomic site occupancies for extra-framework positions, and the isotropic displacement parameters has been performed with the aid of soft constraints (with an initial weight of 10 000) on the tetrahedral bond lengths, used as additional observations in the earlier stages of the refinement and progressively reduced to zero. The scattering curve of Si only was used for the refinement of the tetrahedral atomic sites. It is unrealistic to use mixed Si + Al scattering curves instead of the curve of Si only because the difference in the contribution to the diffraction intensities would have been too subtle and negligible in the refinement system of such a complex structure using X-ray powder diffraction data. The extra-framework ions and water molecules were located by comparison with the extra-framework cation positions in the ECR-1 structure and by using Fourier difference maps. Many extra-framework positions showed partial occupancy. The population of those sites hosting water molecules refined to a value close to 100% was not fixed because it may be an indication of the presence of some disordering and possibly partial ion substitutions.

Figure 4 shows an example of the observed (crosses) and calculated (continuous line) patterns, and difference curve (bottom line) of the refinement, relative to the first data set collected at the GILDA beamline after the background subtraction, in the range $1\text{--}30^\circ 2\theta$. Table 3 is a summary of the refinement statistics and main structural data. Table 4 reports the refined structural data of the framework and extra-framework content. Table 5 reports the calculated bond lengths and angles of direnzoite.

RESULTS AND DISCUSSION

The structures of direnzoite and the isotopic synthetic ECR-1 are composed of layers of mordenite (MOR) and mazzite (MAZ) connected in a regular 1:1 stacking sequence (Fig. 5) with assigned framework topology EON. A comparison of the main structural and chemical data is given in Table 6.

Direnzoite framework density is $16.8 \text{ T}/1000\text{\AA}^3$ with topological density $\text{TD}_{10} = 873$, and $\text{TD} = 0.769676$. The zeolite secondary building unit is 5-1 with ring sizes of 12, 8, 6, 5, 4, and a 2-dimensional channel system. Zeolite maximum diameter of a sphere (<http://www.iza-structure.org/databases/Atlas/freespheres.html>) that can be included in the framework = 7.77 \AA , diffuse along $a = 6.73 \text{ \AA}$, diffuse along $b = 3.18 \text{ \AA}$, diffuse along $c = 1.58 \text{ \AA}$.

The composition of direnzoite determined from the structure refinement is:

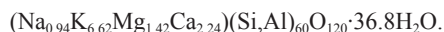


TABLE 3. Structure refinement statistics

Refinement parameter	Value
Total number of data points	9134
Merged $R(F^2)$, no. of observations	10.99%, 5931
Merged χ^2 , no. of refined variables	3.78, 189
Merged R_{wp}	3.99%
Merged R_p	2.87%
Merged R_{wp} (background subtracted)	9.28%
Merged R_p (background subtracted)	4.83%
Merged Durbin Watson Statistics	0.919
a (Å)	7.57887(18)
b (Å)	18.20098(57)
c (Å)	26.15387(83)

The simplified formula is $\text{NaK}_6\text{MgCa}_2(\text{Al}_{13}\text{Si}_{47}\text{O}_{120})\cdot 36\text{H}_2\text{O}$ that corresponds to a molar composition of Na_2O 0.67, K_2O 6.14, MgO 0.88, CaO 2.44, Al_2O_3 14.40, SiO_2 61.37, H_2O 14.10 (Total 100.00 wt%). Except for the K^+ ion content, the agreement with the formula calculated from the EPMA chemical is good (Table 6). A slight overestimation of the K^+ content determined from the Rietveld refinement is plausible because the refined site populations may also account for minor Sr^{++} and Ba^{++} that can occur in the same sites. On the other hand, the K^+ content determined with the EPMA was presumably underestimated because of K^+ migration under the electron beam.

Figure 6 represents the calculated framework of the zeolite structure down the a axis. Direnzoite displays a system of channels with 4-, 5-, 6-, 8-, and 12-membered tetrahedral rings. The widest channel (12-membered of $6.6 \times 7.4 \text{ \AA}$) is along the a axis. Table 5 also reports the average T-O distances and the calculated percentage of Al in that site assuming Al-O distances of 1.746 \AA and Si-O distances of 1.600 \AA . Al-site occupancy is rather similar for T1–T6 sites as it ranges from about 32 to 49%. On the other hand, sites T7–T10 are almost fully occupied by Si as Al site population ranges from about 1 to 10%.

Table 5 shows that some tetrahedral O-T-O angles (O5-T1-O5, O8-T4-O8, O8-T4-O13, O6-T5-O9, O15-T7-O17,

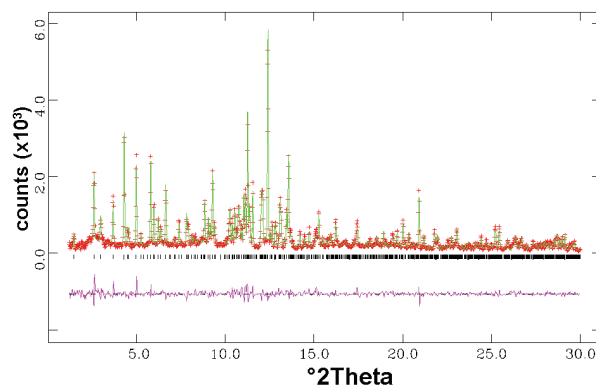


FIGURE 4. The selected $1\text{--}30^\circ 2\theta$ range of the data set collected at the GILDA beamline, showing the background subtracted observed (crosses) and calculated (continuous line) patterns, plus the relative difference curve (bottom line).

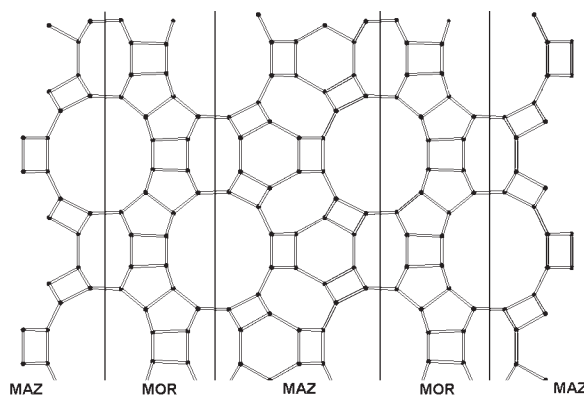


FIGURE 5. The structure of direnzoite with mordenite (MOR) and mazzite (MAZ) layers connected in a regular 1:1 stacking sequence.

TABLE 4. Atomic coordinates, occupancy, and atomic displacement parameters for direnzoite

Site	x/a	y/b	z/c	Site population	U_{iso}^{\dagger} (Å ²)
T1(Si/Al*)	-0.25	0.15917(17)	-0.00519(14)	1	0.017(6)
T2(Si/Al*)	-0.25	0.07632(18)	0.10297(21)	1	0.017(6)
T3(Si/Al*)	-0.25	0.15851(16)	0.21054(17)	1	0.017(6)
T4(Si/Al*)	0.04716(11)	0.16887(21)	-0.09235(31)	1	0.017(6)
T5(Si/Al*)	0.05351(22)	-0.02727(32)	0.14743(24)	1	0.017(6)
T6(Si/Al*)	0.04478(34)	0.05500(19)	0.24977(41)	1	0.017(6)
T7(Si/Al*)	0.25	0.16917(27)	0.40021(36)	1	0.017(6)
T8(Si/Al*)	0.25	0.16590(44)	0.52188(35)	1	0.017(6)
T9(Si/Al*)	-0.04543(17)	0.05520(27)	0.36417(38)	1	0.017(6)
T10(Si/Al*)	0.04706(25)	-0.05395(41)	0.45362(29)	1	0.017(6)
O1	-0.25	0.25	0.01306(21)	1	0.014(5)
O2	-0.25	0.10969(34)	0.04540(72)	1	0.014(5)
O3	-0.25	0.14311(16)	0.14804(38)	1	0.014(5)
O4	-0.25	0.25	0.21987(25)	1	0.014(5)
O5	-0.08536(22)	0.14050(14)	-0.04385(41)	1	0.014(5)
O6	-0.08090(35)	0.02192(19)	0.11231(41)	1	0.014(5)
O7	-0.06629(52)	0.13244(55)	0.23690(28)	1	0.014(5)
O8	-0.01703(44)	0.25	-0.11638(62)	1	0.014(5)
O9	-0.02128(31)	-0.00640(36)	0.20486(53)	1	0.014(5)
O10	0.25	0.15049(12)	-0.07257(40)	1	0.014(5)
O11	0.25	-0.00061(11)	0.12986(25)	1	0.014(5)
O12	0.25	0.07925(36)	0.24525(28)	1	0.014(5)
O13	0.00266(18)	0.11603(30)	-0.14215(51)	1	0.014(5)
O14	-0.01502(24)	0.02533(38)	0.30641(45)	1	0.014(5)
O15	0.25	0.25	0.37502(17)	1	0.014(5)
O16	0.25	0.25	0.54114(35)	1	0.014(5)
O17	0.25	0.15537(41)	0.46062(62)	1	0.014(5)
O18	0.09305(24)	0.12202(37)	0.37500(46)	1	0.014(5)
O19	0.07556(51)	0.12495(29)	0.54309(37)	1	0.014(5)
O20	0.01799(27)	-0.01390(58)	0.39874(46)	1	0.014(5)
O21	0	0	0.5	1	0.014(5)
O22	-0.25	0.05489(33)	0.37670(52)	1	0.014(5)
O23	-0.25	0.07432(26)	0.54272(61)	1	0.014(5)
K1	0.0	0.0	0.0	0.62(4)	0.109(7)
K2	0.25	0.75	0.44103(53)	0.58(6)	0.093(8)
K3	0.25	0.10243(52)	0.72780(50)	0.59(5)	0.116(7)
Na	0.25	0.25	0.27888(44)	0.47(8)	0.026(5)
Ca	0.10841(77)	0.65747(65)	0.31287(52)	0.28(7)	0.100(9)
Mg	0.25	0.25	0.09106(57)	0.72(5)	0.035(7)
H ₂ O1(O)	-0.01826(79)	0.25	0.10661(86)	0.86(4)	0.023(8)
H ₂ O2(O)	0.25	0.11005(88)	0.02455(72)	0.99(3)	0.096(7)
H ₂ O3(O)	0.49895(90)	0.25	0.30815(93)	1.11(6)	0.023(8)
H ₂ O4(O)	-0.04389(76)	0.75	0.36633(80)	1.09(5)	0.113(7)
H ₂ O5(O)	0.25	0.14169(77)	0.12275(85)	0.97(4)	0.050(8)
H ₂ O6(O)	0.75	0.25	0.45418(71)	0.52(6)	0.117(8)
H ₂ O7(O)	0.25	0.25	0.18582(75)	0.75(5)	0.038(7)
H ₂ O8(O)	0.25	0.25	0.00702(79)	1.06(7)	0.136(8)
H ₂ O9(O)	0.50220(65)	0.75	0.22445(79)	1.04(4)	0.102(9)
H ₂ O10(O)	0.75	0.65040(93)	0.33093(70)	0.40(3)	0.157(9)
H ₂ O11(O)	0.75	0.25	0.35258(76)	1.07(7)	0.088(8)
H ₂ O12(O)	0.75	-0.18101(84)	0.24579(73)	0.40(6)	0.149(9)
H ₂ O13(O)	0.25	0.75	0.2856(65)	1.01(2)	0.050(6)
H ₂ O14(O)	0.25	0.6556(26)	0.2231(55)	0.43(2)	0.025(7)

* Only the scattering curve of Si was used in the refinement of the T site.

† An overall atomic displacement parameter was refined for the framework atomic species. Extra-framework species were not constrained.

O18-T7-O18, O18-T9-O22, and O20-T9-O22) are strongly distorted. Apparently no relationship with the Si/Al content of the tetrahedra is found. Besides, only O5, O6, and O15 out of all the framework O atoms involved in these joints are coordinated to extra-framework cations that may act as stretching agent. Thus, we believe that such distortion may simply be an artifact of such a complex structure refinement especially if one considers that soft constraints on the tetrahedral bond lengths, used as additional observations in the earlier stages of the refinement, were reduced to zero in the final stage of the refinement.

Six extra-framework sites and 14 distinct sites for the water molecules were determined in direnzoite. Three extra-framework

TABLE 5. Calculated interatomic distances (Å) and angles (°) of direnzoite

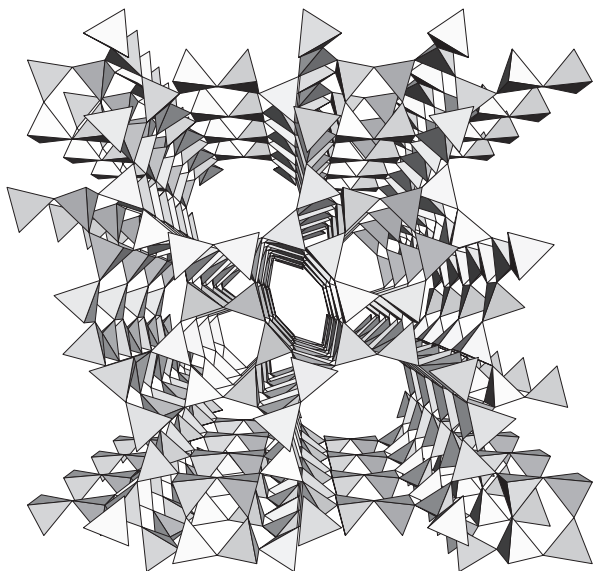
Framework		Extra-framework	
T1-O1	1.721(5)	T5-O13	1.676(5)
T1-O2	1.600(4)	Mean T5-O	1.651
T1-O5	1.642(3) × 2	%Al*	34.93
Mean T1-O	1.651	O6-T5-O9	99.8(2)
%Al*	34.93	O6-T5-O11	103.8(2)
O1-T1-O2	108.1(2)	O6-T5-O13	108.8(1)
O1-T1-O5	111.7(4) × 2	O9-T5-O11	119.7(3)
O2-T1-O5	113.1(1) × 2	O9-T5-O13	102.1(3)
O5-T1-O5	98.9(2)	O11-T5-O13	120.4(3)
T2-O2	1.623(4)	T6-O7	1.676(4)
T2-O3	1.693(4)	T6-O9	1.697(3)
T2-O6	1.638(3) × 2	T6-O12	1.621(4)
Mean T2-O	1.648	T6-O14	1.640(4)
%Al*	32.87	Mean T6-O	1.658
O2-T2-O3	112.1(2)	%Al*	39.72
O2-T2-O6	111.4(3) × 2	O7-T6-O9	105.5(2)
O3-T2-O6	109.3(4) × 2	O7-T6-O12	103.8(2)
O6-T2-O6	103.0(2)	O7-T6-O14	108.6(3)
T3-O3	1.659(5)	O9-T6-O12	114.3(4)
T3-O4	1.683(5)	O9-T6-O14	109.1(4)
T3-O7	1.624(3) × 2	O12-T6-O14	114.9(3)
Mean T3-O	1.647	T7-O15	1.612(4)
%Al*	32.19	T7-O17	1.600(5)
O3-T3-O4	108.1(2)	T7-O18	1.608(3) × 2
O3-T3-O7	111.6(4) × 2	Mean T7-O	1.607
O4-T3-O7	103.1(4) × 2	%Al*	4.79
O7-T3-O7	118.0(2)	O15-T7-O17	123.2(3)
T4-O5	1.698(3)	O15-T7-O18	108.6(3) × 2
T4-O8	1.677(4)	O17-T7-O18	108.7(1) × 2
T4-O1	1.656(3)	O18-T7-O18	95.4(2)
T4-O13	1.654(4)	T8-O16	1.611(5)
Mean T4-O	1.671	T8-O17	1.614(5)
%Al*	48.63	T8-O19	1.616(3) × 2
O5-T4-O8	112.1(1)	Mean T8-O	1.614
O5-T4-O10	104.7(2)	%Al*	9.59
O5-T4-O13	106.9(2)	O16-T8-O17	115.0(3)
O8-T4-O10	124.3(3)	O16-T8-O19	109.3(3) × 2
O8-T4-O13	99.1(2)	O17-T8-O19	106.6(2) × 2
O1-T4-O13	108.5(1)	O19-T8-O19	109.8(2)
T5-O6	1.638(3)	T9-O14	1.622(4)
T5-O9	1.650(4)	T9-O18	1.631(3)
T5-O11	1.639(3)	T9-O20	1.622(3)
Extra-framework			
K1-O2	3.00(5) × 2	Ca-H ₂ O4	2.47(5)
K1-O5	2.88(3) × 2	Ca-H ₂ O9	2.98(6)
K1-O6	3.03(4) × 2	Ca-H ₂ O10	2.76(6)
K1-H ₂ O2	2.83(5) × 2	Ca-H ₂ O13	2.12(5)
K2-O19	3.38(3) × 4	Ca-H ₂ O14	2.58(5)
K2-O23	3.22(3) × 2	Mg-H ₂ O1	2.07(5) × 2
K2-H ₂ O4	2.96(4) × 2	Mg-H ₂ O5	2.14(6) × 2
K2-H ₂ O6	2.74(4)	Mg-H ₂ O7	2.48(3)
K3-O9	3.03(5) × 2	Mg-H ₂ O8	2.20(4)
K3-O14	3.06(3) × 2		
K3-H ₂ O9	3.51(2) × 2		
K3-H ₂ O10	1.77(4)		
K3-H ₂ O12	1.59(4)		
Na-O15	2.51(2)		
Na-H ₂ O3	2.04(4) × 2		
Na-H ₂ O7	2.43(2)		

* See text for details.

sites are occupied by K⁺ ions with Na⁺, Ca⁺⁺, and Mg⁺⁺ distributed over three other distinct sites (see Fig. 7). All the extra-framework sites display partial occupancy. K1 was refined at the origin, inside the 8-ring channels of the MAZ sheet with eightfold coordination with 6 framework O atoms and 2 water molecules (H₂O2) at average distance of 2.935 Å. K2 is located within the large 12-ring channel of the MOR sheet at the window formed by the 8-membered ring with ninefold coordination with 6 framework O atoms and 3 water molecules (2 H₂O4 and 1 H₂O6) at average distance of 3.18 Å. K3 is found within the 12-ring

TABLE 6. Comparison of direnzoite and synthetic zeolite ECR-1 from the Rietveld structure refinement

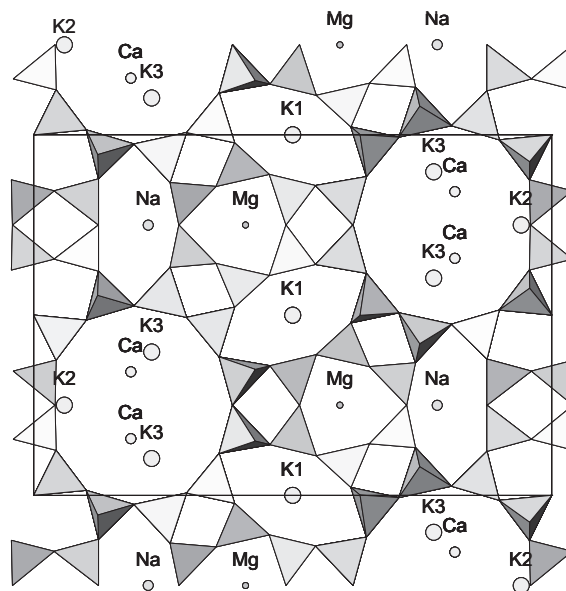
	Direnzoite	ECR-1
Space group	<i>Pmmn</i>	<i>Pmmn</i>
Cell parameters	$a = 7.57887(18) \text{ \AA}; b = 18.20098(57) \text{ \AA}; c = 26.15387(83) \text{ \AA}$	$a = 7.5675(1) \text{ \AA}; b = 18.1187(4) \text{ \AA}; c = 26.0605(7) \text{ \AA}$
Cell volume (<i>V</i>)	3607.74 (18) \AA^3	3573.2(5) \AA^3
Calculated chemical formula	$(\text{Na}_{0.94}\text{K}_{6.62}\text{Mg}_{1.42}\text{Ca}_{2.24})(\text{Si,Al})_{60}\text{O}_{120}\cdot 36.8\text{H}_2\text{O}$	$(\text{Na}_{10.97}\text{Ca}_{0.36})(\text{Si,Al})_{60}\text{O}_{120}\cdot 35.0\text{H}_2\text{O}$

**FIGURE 6.** The framework of the zeolite structure down the *a* axis.

channel close to the bottom 6-membered ring. It has eightfold coordination environment with 4 framework O atoms and 2 water molecules (H_2O_9) at average distance of 3.2 \AA . Calcium is also found within the 12-ring channel close to the positions labeled H in the compilation of extra-framework sites for mordenite (Mortier 1982). Calcium has a distorted pyramid-like fivefold coordination with five water molecules (H_2O_4 , H_2O_9 , H_2O_{10} , H_2O_{13} , and H_2O_{14}) at average distance of 2.58 \AA . Sodium is found within the 8-ring channels of the MOR sheet with fourfold coordination environment with one framework O atoms and 3 water molecules ($2 \times \text{H}_2\text{O}_3$ and H_2O_7) at average distance of 2.255 \AA . Its position is approximately equivalent to the position labeled A sites (Mortier 1982) for mordenite and usually occupied by Na atoms. Like in mazzite, Mg is found at the center of the gmelinite cage, totally surrounded by water molecules and with no contact to the framework O atoms (type IV cation site: Galli 1975). Magnesium has sixfold coordination with average Mg- H_2O distance of 2.183 \AA .

The extra-framework cation distribution is fairly different from that calculated for ECR-1. In direnzoite, there are no equivalent positions to C1, C2, and C4 positions found in ECR-1. Only sites C3 and C3b correspond respectively to K3 and Ca in direnzoite. In direnzoite, K1, K2, and Na correspond to water molecules sites (H_2O_1 , H_2O_{11} , and H_2O_8 , respectively) in ECR-1.

Concerning the origin of this new zeolite species, hydrothermal crystallization within the pores and cavities of the highly porphyric basalt is postulated. It is interesting to speculate over the origin of direnzoite and the reasons because neither mordenite nor mazzite formed. Note that all the three zeolite species have fibrous habit. One reason should certainly be the

**FIGURE 7.** The distribution of the cations and water molecules in direnzoite viewed down [100]. The plotted unit cell is shifted by 0,0,1/2 relative to the coordinates given in Table 4.

Si/Al ratio in the crystallization environment, which has to be unusual given the rarity of direnzoite. The calculated R (=Si/Si + Al) value of direnzoite is 0.778. This value is just in between those observed for the formation of both natural and synthetic mordenite (0.80–0.86) and mazzite (0.72–0.75) (Passaglia and Sheppard 2001). Moreover, although the crystallization conditions may have played in favor of mordenite formation, the presence of Mg, acting as templating agent, should favor the crystallization of mazzite. In contrast, the presence of Na in solution likely inhibited the formation of mazzite and favored the crystallization of mordenite because Na-rich mazzite specimens have only been reported in the literature as a product of secondary Na-cation exchange in contact with Na-rich fluids (see Na-mazzite from Boron, California: Arletti et al. 2005). The result of these unique chemical environments between that typical of mordenite and mazzite, prompted the crystallization of direnzoite with a structure composed of mordenite and mazzite sheets. With respect to the natural species, both the crystallization of zeolite Ω (omega), the synthetic isotype of mazzite, and the crystallization of the synthetic isotype of direnzoite, ECR-1 require the use of tetramethylammonium (TMA) as an organic templating agent (Barrer and Villiger 1969; Galli et al. 1974; Gualtieri et al. 2006).

To the knowledge of the authors, this is one of the few examples of a natural zeolite structure solved using powder methods. In the past, the structure of only four other natural zeolites was solved using powder methods: (1) gobbinsite (McCusker et

al. 1985); (2) montesommaite (Rouse et al. 1990); (3) perliolite (Artioli and Kvik 1990); and (4) garronite (Artioli 1992). The solution of the structure of direnzoite was made possible because it is the K-dominant equivalent of the synthetic zeolite ECR-1 with a structure composed of layers of mordenite (MOR) and mazzite (MAZ) connected in a regular 1:1 stacking sequence.

ACKNOWLEDGMENTS

S. Ferrari is greatly acknowledged for his help during the preliminary steps of this project. Thanks are due to C. Meneghini for the help during the synchrotron experiment performed at beamline BM08 (ESRF). We also thank W. van Beek and H. Emerich for help during the synchrotron data collections at beamline BM01 (SNBL/ESRF). M. Tonelli is kindly acknowledged for the collection of the SEM images. A. Tombesi is acknowledged for the collection of the FTIR patterns. G. Chiari is greatly acknowledged for useful discussions. M. Lassinantti Gualtieri is also acknowledged for the reading of the manuscript. Finally, we thank the Associate Editor D. Gatta and the two competent referees M. Gunter and R.X. Fisher for their careful revision, which improved the quality of the manuscript.

REFERENCES CITED

- Amemija, Y. (1990) Imaging plate X-ray area detector based on photostimulable phosphor. *Synchrotron Radiation News*, 3, 21–26.
- Arletti, R., Galli, E., Vezzali, G., and Wise, W.S. (2005) Mazzite-Na, a new zeolite from Boron, California: Its description and crystal structure. *American Mineralogist*, 90, 1186–1191.
- Armbruster, T. and Gunter, M.E. (2001) Crystal structures of natural zeolites. In D.L. Bish and D.W. Ming, Eds., *Natural Zeolites: Occurrence, Properties, Applications*, 45, p. 1–68. Reviews in Mineralogy and Geochemistry, Mineralogical Society of America, Chantilly, Virginia.
- Artioli, G. (1992) The crystal structure of garronite. *American Mineralogist*, 77, 189–196.
- Artioli, G. and Kvik, A. (1990) Synchrotron X-ray Rietveld study of perliolite, the natural counterpart of synthetic zeolite-L. *European Journal of Mineralogy*, 2, 749–759.
- Barrer, R.M. and Villiger, H. (1969) The crystal structure of the synthetic zeolite L. *Zeitschrift für Kristallographie*, 128, 352–370.
- Brousse, R. (1961) Mineralogie e petrographie des roches volcaniques du Massif du Mont Dore (Auvergne). *Bulletin Societé Française de la Mineralogie Cristallographie*, 84, 131–186.
- Galli, E. (1975) Crystal structure refinement of mazzite. *Rendiconti Società Italiana di Mineralogia e Petrologia*, 31, 599–612.
- Galli, E., Passaglia, E., and Pongiluppi, D. (1974) Mazzite, a new mineral, the natural counterpart of the synthetic zeolite. *Contribution to Mineralogy and Petrology*, 45, 99–105.
- Gottardi, G. and Galli, E. (1985) *Natural Zeolites*, 409 p. Springer Verlag, Berlin.
- Gualtieri, A.F., Ferrari, S., Galli, E., Di Renzo, F., and van Beek, W. (2006) Rietveld structure refinement of zeolite ECR-1. *Chemistry of Materials*, 18, 76–84.
- Hammersley, A.P. (1998) FIT2D V10.3 Reference Manual V4.0 ESRF98HA01T. ESRF, Grenoble, France.
- Larson, A.C. and Von Dreele, R.B. (2000) General structure analysis system (GSAS). Los Alamos National Laboratory, document LAUR 86–748.
- McCusker, L.B. and Baerlocher, C. (1985) Rietveld refinement of the crystal structure of the new zeolite mineral gobbsinite, Locality: County Antrim, Northern Ireland. *Zeitschrift für Kristallographie*, 171, 281–289.
- Meneghini, C., Artioli, G., Balerna, A., Gualtieri, A.F., Norby, P., and Mobilio, S. (2001) Multipurpose imaging-plate camera for in situ powder XRD at the GILDA beamline. *Journal of Synchrotron Radiation*, 8, 1162–1166.
- Mortier, W.J. (1982) *Compilation of extra framework sites in zeolites*. Butterworths, Guildford, England.
- Passaglia, E. (1970) The crystal chemistry of chabazites. *American Mineralogist*, 55, 1278–1301.
- Passaglia, E. and Sheppard, R.A. (2001) The crystal chemistry of zeolites. In D.L. Bish and D.W. Ming, Eds., *Natural Zeolites: Occurrence, Properties, Applications*, 45, p. 70–116. Reviews in Mineralogy and Geochemistry, Mineralogical Society of America, Chantilly, Virginia.
- Rouse, R.C., Dunn, P.J., Grice, J.D., Schlenker, J.L., and Higgins, J.B. (1990) Montesommaite, $(K,Na)_9Al_9Si_{23}O_{64} \cdot 10H_2O$, a new zeolite related to merlinoite and the gismondine group. *American Mineralogist*, 75, 1415–1420.
- Toby, B.H.J. (2001) EXPGUI, a graphical user interface for GSAS. *Journal of Applied Crystallography*, 34, 210–213.
- Warrender, S.J., Wright, P.A., Zhou, W., Lightfoot, P., Camblor, M.A., Shin, C.H., Kim, D.J., and Hong, S.B. (2005) TNU-7: A large-pore gallosilicate zeolite constructed of strictly alternating MOR and MAZ layers. *Chemistry of Materials*, 17, 1272–1274.

MANUSCRIPT RECEIVED APRIL 11, 2007

MANUSCRIPT ACCEPTED SEPTEMBER 6, 2007

MANUSCRIPT HANDLED BY G. DIEGO GATTA